Hindawi
International Journal of Antennas and Propagation
Volume 2022, Article ID 6741689, 15 pages
https://doi.org/10.1155/2022/6741689

Research Article

Impact of Various Wearability Conditions on the Performances of Meander-Line *Z*-Shaped Embroidered Antenna

Adnan E. Ali, Goran M. Stojanović, Varun Jeoti, Dalibor Sekulić, and Ankita Sinha

Faculty of Technical Sciences, University of Novi Sad, T. Dositeja Obradovica 6, Novi Sad 21000, Serbia

Correspondence should be addressed to Goran M. Stojanović; sgoran@uns.ac.rs

Received 1 September 2022; Revised 4 October 2022; Accepted 10 October 2022; Published 25 October 2022

Academic Editor: Trushit Upadhyaya

Copyright © 2022 Adnan E. Ali et al. This is an open access article distributed under the Creative Commons Attribution License, which permits unrestricted use, distribution, and reproduction in any medium, provided the original work is properly cited.

The field of wearable computing technology describes the future of electronic systems being an integral part of our everyday clothing with various enhanced functionalities. The present work is aimed at making closer steps towards the real wearability of electronics using textiles. We designed a fully-textile meander line *Z*–shaped monopole antenna for radio-frequency (RF) harvesting and for short-range communication purposes in the body-area network for various wearable applications. The target antenna was designed in the Ansys HFSS software tool and fabricated on a single-layer cotton textile using silver conductive threads and an embroidery technique. The antenna was characterized using a vector network analyzer (VNA), and the selected design was found to be nearly invariant under different deployment conditions. Antenna performance was studied by measuring the return loss while the antenna was in close proximity to the human body, or under various bending scenarios and/or wet conditions with sweat. The simulated return loss was −20.36 dB at an operating frequency of 1.62 GHz, and the measured return loss for the fabricated antenna was −19.45 dB at 1.6275 GHz with a −10 dB bandwidth of 100 MHz (i.e., 1.58 GHz to 1.68 GHz), and a fractional bandwidth of 6.17%. The results of this study are very important for the design of future wearable antennas in the new concept of the Internet of bodies.

1. Introduction

In today's world, wearable and flexible wireless technologies have a significant role in effective communication and are one of the hottest trends that aim at interweaving technology into everyday activities to maximize the quality of life for human beings [1, 2]. This interconnection of electronic components and other materials such as fabrics introduced a new concept, so-called wearable smart textiles or e-textiles, which have expanded functionality and performance to be more application specific. Due to the advancement in technology, the demand for smart interactive textile systems has increased in the military, sports, consumer electronics, as well as medical sectors [3, 4]. However, one of the main challenges that limit the successful implementation and commercialization of such technologies is the power supply. Conventional batteries make the system too bulky and obtrusive. On the other hand, energy harvesting introduces attractive features, such as self-sustainability and environmental friendliness, which makes it suitable to be used in a wide area of applications such as human-body-centric communication and sensing systems. These applications require the easy integration of flexible and textile-based high-data-rate wireless electronic devices into clothing and other wearable devices so that the wearer can easily communicate with different devices. Given that these systems are designed to be applicable for various daily activities, the integrated components should maintain a reliable link without any discomfort to the user, and hence, not be obtrusive. The additional requirement imposed on wearable and body-worn systems is that the used materials should be biocompatible and compliant with the health and safety requirements [5, 6]. Since the antenna is an inherent and integral part of any wireless communication [7] and radio-frequency (RF) harvesting system, there is a considerable interest in the optimization of wearable and flexible antennas and radio-channel for operation in the vicinity of the human body [8]. However, in the presence of the human

body, which is a lossy dielectric, the performance of any flexible antenna is unduly affected. The design challenges of a wearable antenna, intended to be deployed on-body, have to largely do with keeping the degradation in the performance of the antenna within an acceptable range of performance.

The research activities in the area of antennas for body-centric and other various wearable applications are focused on the design of flexible and conformable antennas that are technically suitable and aesthetically acceptable to be worn on the human body [9–12]. Various effective and interesting techniques, such as planar inverted antennas, the use of high relative permittivity materials, and meander-line designs, were proposed [13–15] for the miniaturization of antennas and enhancement of bandwidth. Meander-line technology allows us to achieve a reduction in the size of antennas by combining a set of horizontal and vertical lines and folding them back and forth at right angles to maintain a reduction in the overall antenna length [16, 17]. Wearable antennas are required to have good radiation characteristics performance and operating frequency, depending on the application requirements when placed in proximity to the human body [18]. However, in real conditions, these antennas will be subject to bending and can come into direct contact with ionically conducting bodily liquids. Compared to other biofluids such as blood, urine, and breath, sweat can be sampled noninvasively and the collected information can be used for monitoring species of interest, particularly in the criminal justice system. As a result, there is a need to develop an easy-to-use and less invasive wearable antenna, whose properties do not change when mounted on body-worn garments.

Previous antenna-human interaction research has focused on designing wearable antennas that are planar, low-profile, light-weight, and flexible to suit the conformal structure of the body [8, 18, 19]. Various feeding techniques were also adopted to energize these antennas, including microstrip-line feed, coaxial feeding, as well as coplanar waveguide feeding methods [15]. Different flexible dielectric substrates such as Kapton, polydimethylsiloxane (PDMS), liquid crystal polymer (LCP), polytetrafluoroethylene (PTFE), polyimides (PI), and paper-based substrates [20–25] have been proposed in the open literature. However, since wearable antennas are required to be directly integrated with the clothes, the components used should be made of suitable materials to achieve proper radiation characteristics while maintaining the functionality of the textile itself. This gives rise to the utilization of textiles as a substrate and conductive textile threads [26, 27] as a wire for designing wearable antennas. Commonly used textile dielectric materials include cotton cloth, felt, denim, fleece, nylon, and polyester [8, 28]. Numerous flexible and wearable antennas were designed and fabricated using different techniques such as 3D printing, inkjet-printing, embroidery, and screen-printing [20, 29]. Compared to other manufacturing methods, embroidery is the most preferable and cost-effective technique for textile antennas. An integrated planar monopole antenna was designed and fabricated in [13, 30], using Pellon fabric as a substrate and pure copper taffeta for the conducting parts. Different textile-based antennas were also studied in [30–32], where the ground plane and the patch were designed on different planes and a number of additional layers were sandwiched in between them to get the required substrate thickness. Bending and crumpling conditions were also studied for the fabricated antennas, where their performance showed a considerable change in the resonant frequency.

This paper purposes a coplanar waveguide- (CPW-) fed embroidered *Z*-shaped meander line monopole wearable textile antenna for radio-frequency (RF) harvesting and for short-range communication in the body-area network for various wearable applications. The antenna was designed to operate at 1.62 GHz and was fabricated on a single-layer cotton textile dielectric substrate without using any additional rigid electronic components or adhesive materials. Another novelty of the proposed antenna lies in its fabrication where conducting parts were made only on one-side of the dielectric substrate, which makes the target antenna highly conformal, ergonomic, and flexible to accommodate daily human movement. To simulate the functionality of a fabricated antenna in the real environment, its performance was investigated using a vector network analyzer by means of measurement of the return loss when placed in proximity to the human body, under bending scenarios, and repeated wet conditions with sweat, which is very limited in the open literature.

The rest of this article is organized as follows. After the introduction, Section 2 describes the materials required and techniques employed, followed by design steps and simulations, as well as fabrication and validation of the proposed antenna. In Section 3, brief discussions on the simulations, measurement setup, and results obtained in terms of the input-return loss, voltage standing wave ratio, bandwidth, and other antenna parameters under different deployment and wearability conditions are presented. Finally, conclusions drawn from the obtained results are summarized and future research directions on flexible antennas for high-frequency body-area network applications are highlighted.

2. Materials and Methods

In this section, the materials required and techniques employed follow the design methodology; configuration and parameter estimations, as well as fabrication and validation of the proposed antenna, are presented and discussed.

2.1. Materials and Techniques. Due to the ease of integration into clothing and the conformal nature of fabrics, studies of flexible and wearable antennas using textile dielectric materials are becoming more popular compared to conventional rigid substrates [13]. However, in many of these structures, a number of additional layers were stacked between the radiating patch and the ground plane to get the required substrate thickness. The proposed meander line *Z*-shaped antenna was designed and simulated in the ANSYS High-Frequency Structural Simulator (HFSS) software tool using a single-layer cotton textile (relative permittivity: $\varepsilon_r = 1.68$, dielectric loss tangent: $\tan\delta = 0.04$ and substrate thickness: $h = 1.3$ mm). A digital embroidery machine (JCZA

0109-550), manufactured by ZSK Technical Embroidery Systems, Germany, was used for fabricating the proposed wearable antenna on a woven cotton textile substrate without using any additional rigid electronic components or adhesive materials. Commercially available silver coated conductive polyamide/polyester hybrid thread (silver-tech 50 with a nominal resistance of 150 Ω/m and diameter of 0.36 mm), supplied by AMANN GROUP, Germany, was used to create the Z-shaped radiating patch, feedline, and the ground plane conducting parts all in the same plane. A subminiature version-A (SMA) connector of 50 Ω characteristic impedance was carefully attached to the fabricated antenna, using a soldering technique and silver conductive paste. The fabricated textile antenna was characterized using a two-port vector network analyzer (VNA–Agilent E5071B), manufactured by Keysight (formerly known as Agilent Technologies), under different deployment and wearability conditions. Rolling papers with a diameter of 120 mm, 100 mm, 80 mm, and 60 mm were chosen to study the impact of bending on antenna performance and ensure its structural integrity in real wearable and on-body applications. Moreover, to validate the functionality of the fabricated wearable antenna under exposure to different accidental spills, ethanol alcohol (70% v/v), and vodka alcohol (40% v/v) were applied to the conducting parts of the antenna.

2.2. Design Methodology. Selection of the required substrate materials in terms of thickness and dielectric properties, such as loss tangent and relative permittivity, fabrication technique, method of feeding, and overall antenna design structure are important aspects to be considered while designing wearable and flexible antennas. The basic procedure shown in Figure 1 was employed for the design, simulation, as well as optimization of the proposed antenna design parameters.

2.3. Antenna Design and Configuration. The design and simulation of the proposed antenna was performed using the Ansys HFSS Electromagnetics Suite, which is commonly used for designing a broad range of high-frequency electronic components such as antennas, RF or microwave components, and other Internet-of-things (IoT) products. This tool is based on a highly accurate finite element method and other integral equation methods supported by high-performance wearable computing technology to get the required frequency domain solutions. The design of the CPW-fed meander-line *Z*-shaped textile antenna typically consists of the radiating meander-line patch, a dielectric substrate, and two equal sized ground planes with the gap (b) from the feedline as shown in Figure 2. The structure of the antenna is based on a meander-line technology that allows it to achieve miniaturization in size and wideband antenna performance by combining a set of horizontal and vertical lines that form right-angle bends. The efficiency and resonant frequency of a meander-line antenna depend on the number of turns of a meander and the spacing between the meander-lines, respectively [33]. The performance of antenna, such as wider bandwidth, higher resolution, and better radiation, can be enhanced by using thicker substrates with a low dielectric constant (usually less than 6); however, this leads to larger antenna dimensions [34]. Therefore, another mechanism of improving antenna performance by inserting meander-line slots to perturb the flow of current is applied in our design. The main radiator is a microstrip meander-line with two parallel and equal-sized meandered slots that form a *Z*-shape, which is then directly connected to the 50 Ω feedline.

2.4. Analysis of Design Specification. The structure of the antenna is realized by a *Z*-shape meander line with dimensions of L_p and W_p, where L_p is the length of the antenna, W_p is the width of the antenna, and W_m is the width of the meander-line shape. The operating frequency (f_0) and substrate parameters (ε_r, h) are fundamental parameters for the design and simulation of the antenna. The substrate thickness (h = 1.3 mm) is the value obtained by measuring the thickness of the textile substrate together with the embroidered conductive threads. This value is used in the design and simulation process and further calculation of other antenna dimensions. Figure 3 depicts the detailed geometric configuration of the *Z*-shaped meander-line antenna element whose dimensions are calculated in accordance with the operating frequency (f_0) and, hence, the free space wavelength (λ_0). Two parallel meander-line slots of length approximately equal to the width of the antenna (W_p) were placed symmetrically in the XY plane to form the *Z*-shaped radiator element. Initially, the length and width of the radiating patch antenna with the specified relative dielectric constant and thickness of the substrate were calculated. This is then followed by the calculations of the effective relative dielectric constant and the change in the length extension (ΔL) due to fringing effects, as illustrated in Figure 2, between the radiating patch and substrate.

The relative permittivity of the dielectric material, the thickness of the substrate, and the resonant frequency are important design parameters [35] based on which the following dimension calculations were performed for the proposed textile antenna. First, the width (W_p) of the meander-line patch antenna was calculated using the following formula.

$$W_p = \frac{c}{4f_0}\sqrt{\frac{2}{1+\varepsilon_r}}, \tag{1}$$

where $c = 3 * 10^8\, m/s$ is the speed of light in free space, f_0 is the resonant frequency, and ε_r is the relative dielectric permittivity of the cotton substrate material, which is then followed by calculating the value of the effective dielectric constant on the given substrate (for $W_p/h > 1$) as in [36];

$$\varepsilon_{\Re} = \frac{\varepsilon_r + 1}{2} + \frac{\varepsilon_r - 1}{2}\left(1 + 12\frac{h}{W_p}\right)^{-1/2}, \tag{2}$$

where $\varepsilon_{\Re}$ is the effective relative dielectric constant of the substrate, h is the substrate thickness, and W_p is the width of

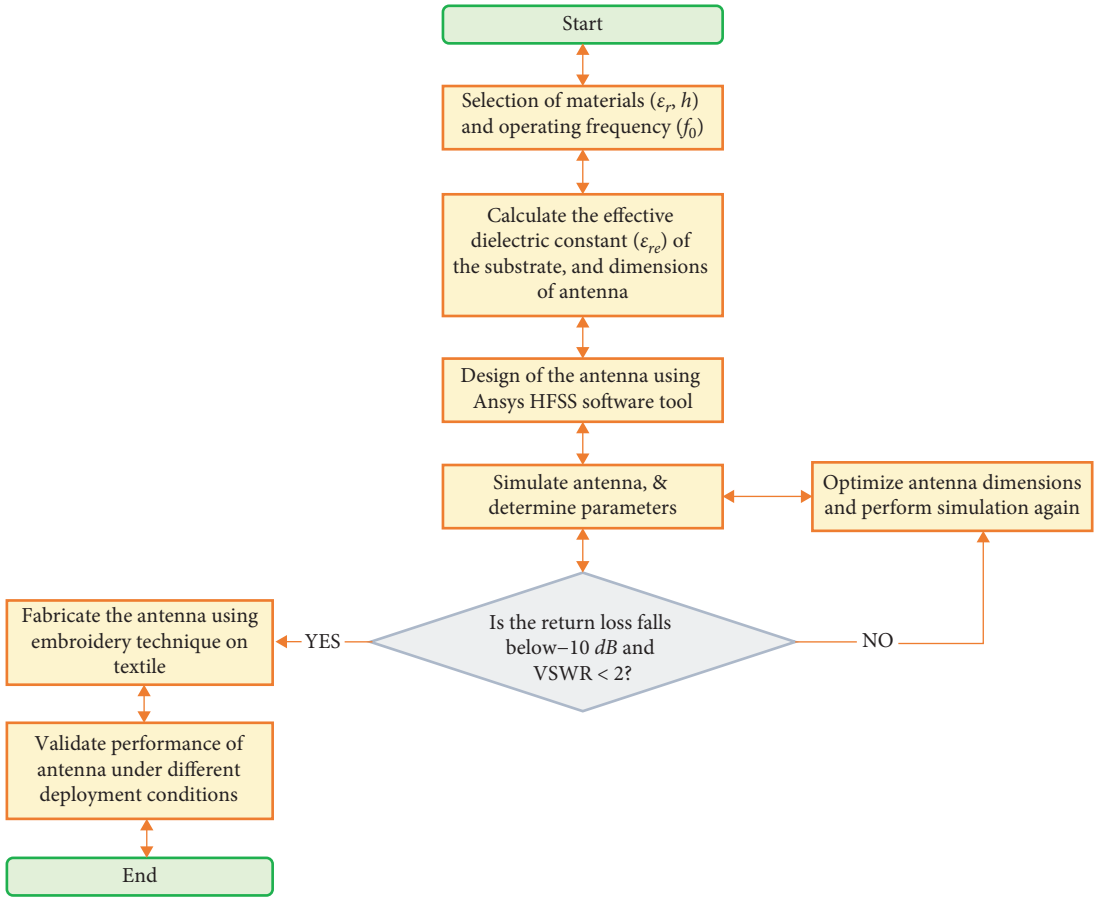

Figure 1: Flowchart for the design of meander-line Z-shaped textile antenna.

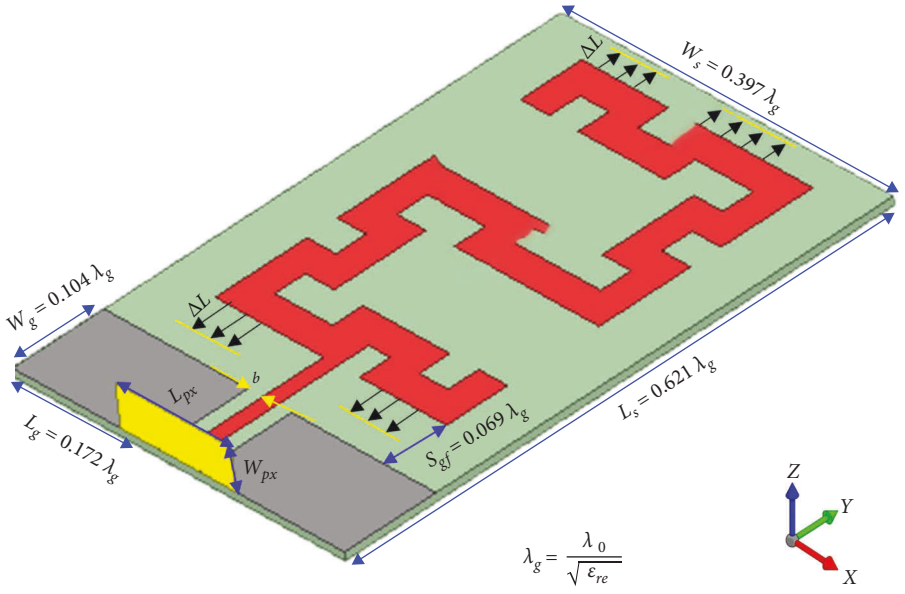

Figure 2: Proposed design of a meander-line Z-shaped monopole antenna.

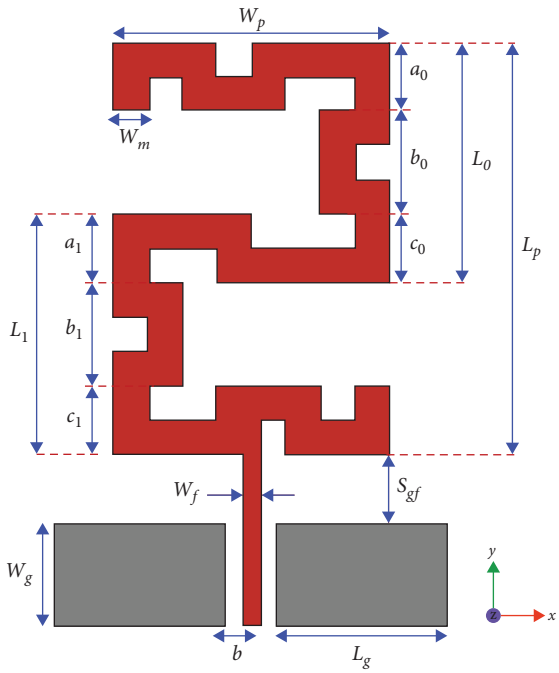

FIGURE 3: Configuration of the designed meander-line Z-shaped antenna.

the radiating Z-shaped patch antenna. Due to the fact that the portion of fringing fields from the radiator patch element to the ground plane are confined within the dielectric substrate and the remaining are spread in the air, the value of effective relative permittivity is smaller $(1 < \varepsilon_{\Re} < \varepsilon_r)$ than the actual dielectric value of the substrate [37]. Due to the inherent narrow bandwidth of the resonant element (i.e., patch), the length of the antenna is a very critical design parameter which governs the resonant frequency. In order to calculate the total length of the radiating patch antenna (L_p), first the length (L_0) as in Figure 3 was calculated using (3) and a value of approximately 35 mm was obtained.

$$L_0 = \frac{c}{4 f_0 \sqrt{\varepsilon_{\Re}}} - 2\Delta L, \tag{3}$$

where ΔL is the change in the length extension of the proposed meander-line antenna. Since the radiating Z-shaped antenna has a finite length and width, the electric fields undergo fringing at the edges. Because of this, electrically, the antenna looks larger than its actual physical dimensions [38]. The radiating patch antenna has been extended by ΔL along its length on each side, as shown in Figure 2. This extension in the length of the antenna (ΔL) is a function of the effective relative dielectric constant $(\varepsilon_{\Re})$ and the width-to-height ratio (W_p/h) and is expressed as in [38];

$$\Delta L = 0.412h \frac{(\varepsilon_{\Re} + 0.3)(W_p/h + 0.264)}{(\varepsilon_{\Re} - 0.258)(W_p/h + 0.8)}. \tag{4}$$

Once the length $(L_0 \cong 35\,mm)$ as shown in Figure 3 was obtained, the two lengths L_0 and L_1 are equal, which implies $L_1 \cong 35\,mm$. Then, the length of the Z-shaped radiating element is adjusted as; $a_0 = a_1 = 10\,mm$, $b_0 = b_1 = 15\,mm$, and $c_0 = c_1 = 10\,mm$ such that the total length of the radiating patch element becomes $L_p = L_0 + b_1 + c_1 = L_1 + b_0 + a_0 = 60\,mm$. Therefore, the length and the width of the Z-shaped patch antenna are optimized close to a quarter wavelength of the resonant frequency (f_0). The width of feedline (W_f) and the gap (b) between the ground and the feedline were calculated for a 50 Ω characteristic impedance (for $W_f/b > 0.35$) as in [39].

$$Z_0 = \frac{30\pi}{\sqrt{\varepsilon_r}} * \frac{b}{W_f + 0.441 * b}. \tag{5}$$

Therefore, to get a characteristic impedance of 50 Ω on the given substrate, one of the two parameters, W_f or b was first fixed to a specific value and the other parameter was computed. Accordingly, the width of the transmission line was fixed at 2.5 mm, and the separation distance (b) was calculated as 2.4 mm to ensure the matching to the 50 Ω. The lumped port was used to excite the proposed antenna and the basic rule for port size definition of the transmission line was applied to determine its dimensions. Accordingly, the length of the port (along the X-axis) was chosen to be at least six times the width of the feedline and five times the height of the substrate along its width, as depicted in Figure 2. Usually, antenna dimensions are expressed in terms of wavelength. The shorter the wavelength and the higher the resonant frequency, the smaller the length of the antenna can be fabricated and vice-versa. The dimensions of the substrate, ground and the distance or height of the antenna from the ground plane were computed in terms of the guided wavelength and optimized dimensions are shown in Figure 2. The wavelength inside the dielectric substrate, or guided wavelength (λ_g), is a function of the ratio of free space wavelength-to-effective dielectric constant [40];

$$\lambda_g = \frac{\lambda_0}{\sqrt{\varepsilon_{\Re}}}, \tag{6}$$

where $\varepsilon_{\Re} = 1.63$ is the effective relative dielectric constant of the textile substrate calculated from (2) by using a $1.3\,mm$ thick cotton textile dielectric material and λ_0 is the free space wavelength corresponding to the frequency of operation (f_0). Therefore, the fundamental antenna equation that relates the wavelength, speed of light and (effective) relative permittivity of a dielectric substrate can be expressed as

$$f_0 = \frac{c}{\lambda_0} = \frac{c}{\lambda_g \sqrt{\varepsilon_{\Re}}}. \tag{7}$$

Table 1 summarizes the overall optimized geometrical antenna parameters, calculated using the above design equations, for the proposed meander-line textile antenna structure, which consists of the Z-shaped radiating element of dimension $(L_p * W_p)$, cotton textile dielectric substrate $(L_s * W_s)$, and two ground planes of equal size $(L_g * W_g)$, where relative permittivity: $\varepsilon_r = 1.68$, dielectric loss tangent: $\tan\delta = 0.04$, substrate thickness $h = 1.3$ mm, and the guided

Table 1: Optimized dimensions for the Z-shaped meander-line patch antenna.

Parameter	Description	Value (mm)
L_p	Length of patch	60
W_p	Width of patch	40
L_S	Length of substrate	90
W_S	Width of substrate	57.5
L_g	Length of ground	25
W_g	Width of ground	15
W_f	Width of feedline	2.5
b	Separation distance	2.4
S_{gf}	Antenna height from ground	10
L_{px}	Port length (along the x-axis)	20
W_{pz}	Port width (along the z-axis)	6.5

wavelength inside the dielectric material (λ_g = 145.05 mm) at the operating frequency of 1.62 GHz.

2.5. Fabrication and Validation. Among various techniques available for the fabrication of textile-based wearable antennas, such as inkjet-printing, screen-printing, and 3D printing, the embroidery technique was chosen because of its high speed, flexibility, and cost-effectiveness. Previous works on feasibility of using digital embroidery and conducting threads to create transmission lines and potentially antennas were investigated in [41, 42]. This technology has proven a more flexible manufacturing technique, especially for flexible and textile antennas and the integration of high-frequency systems into clothing. The proposed meander-line textile antenna was fabricated using a double-head digital embroidery machine, which consists of the F-head (also called standard embroidery) operating at an embroidery speed of 1000 stitches per minute depending on the stitch length and materials used. The designed antenna in Ansys HFSS was exported as a DXF file and later converted into a ZSK TC (Transport Code) file using the GiS BasePac 10 software tool provided by ZSK Technical Embroidery Systems, which is more compatible with an embroidery machine for production. For the creation of antenna, both the conductive and nonconductive threads were used, which are then interloped during the embroidery process, as shown in Figure 4(a), in order to create stitched pattern on the substrate. The top conductive thread (silver thread) runs through a tension system, take-up lever, and the needle eye, which is then pulled along the bottom of the substrate to form the lock stitch. The nonconductive lopper thread (cotton thread) is wound onto the bobbin, which is then inserted into a casing in the lower half of the machine for the proper operation of embroidery in creating the required stitched antenna designs on the textile substrate.

After the fabrication of antenna, a sub-miniature version-A (SMA) connector of 50 Ω characteristic impedance was carefully coupled, using soldering technique and silver conductive paste as shown in Figure 4(b), with the two ground planes and the feed port in order to perform measurements. To validate the simulated design and calculated results, the attached SMA connector was further linked to a two-port VNA, which provides comprehensive measurement capability in the range of frequencies from 300 kHz to 8.5 GHz, through a 50 Ω coaxial cable. An experimental study of antenna performance was conducted by means of the measurement of the reflection coefficient (dB) and other antenna parameters under different deployment and wearability conditions. Figure 4(c) shows the scanning electron microscope (SEM) images of the embroidered textile antenna. The darker area is the cotton textile material and nonconductive thread, and the lighter area shows silver conductive threads.

3. Results and Discussion

This section presents the simulations followed by measurement results for the fabricated textile antenna under different wearability and deployment conditions. The antenna response under the exposure to accidental spills of ethanol alcohol and vodka alcohol, which mimic the realistic on-body situation, are also presented and discussed.

3.1. Simulated and Measured Return Loss and Bandwidth. The simulated design of a wearable Z-shaped antenna on a cotton textile material showed a good return loss result over the frequency range from 0.9 GHz up to 2.4 GHz. In antenna design and simulation, the quality of matching the antenna to the feedline and RF source is specified by the return loss and voltage standing wave ratio (VSWR). The return loss, or S11 (dB), indicates how much power is reflected back to the transmitter from the antenna due to impedance mismatch. The higher the value of S11 (dB), the greater the impedance mismatch between the antenna and transmitter and, consequently, the less forward power feed to the antenna. Similarly, the voltage standing wave ratio is an indication of the amount of mismatch between the antenna and the feed line connected to it. The smaller the value of VSWR (usually $1 < VSWR < 2$), the antenna is better matched to the feedline and more power is delivered to it. Simulation results were validated by means of measurement of the return loss using a VNA–E5071B as shown in Figure 5. An empty box with a rectangular cut (of the same dimension as the antenna under test) was prepared and the fabricated antenna was placed on top of it for measurement purposes.

The simulated and measured return loss (dB) and VSWR plots for the fabricated textile antenna were analysed as depicted in Figures 6(a) and 6(b). The simulated return loss was −20.36 dB at an operating frequency of 1.62 GHz and the measured return loss for the fabricated antenna was −19.45 dB at 1.6275 GHz with a −10 dB bandwidth of 100 MHz (i.e., 1.58 GHz to 1.68 GHz) and a fractional bandwidth of 6.17%. Even though there are slight variations between the simulations and measurement results, which can be attributed to the soldering of a 50 Ω SMA connector to the fabricated textile antenna, the return loss for the fabricated antenna prototype was able to cover the required range of frequencies over which the antenna operates properly. Similarly, the value of VSWR for the antenna falls within the acceptable range. It can be observed from Figures 6(a) and 6(b) that experimental results verify the

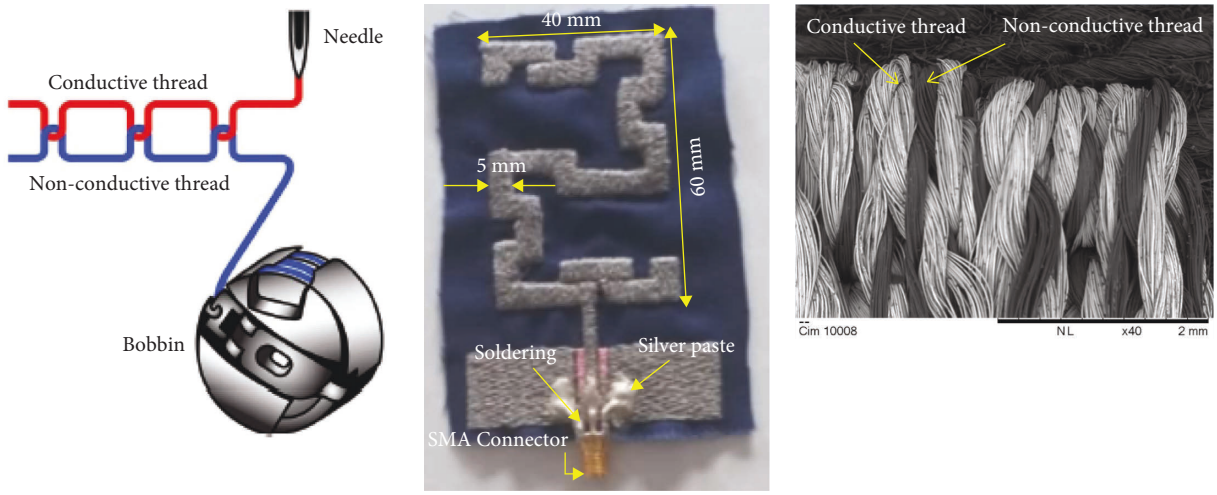

FIGURE 4: (a) Bobbin with top conductive thread and bottom looper thread to be inserted in the lower half of an embroidery machine; (b) fabricated *Z*-shaped meander-line monopole textile antenna; (c) SEM image showing the interlacement of the conductive and nonconductive threads during the embroidery process.

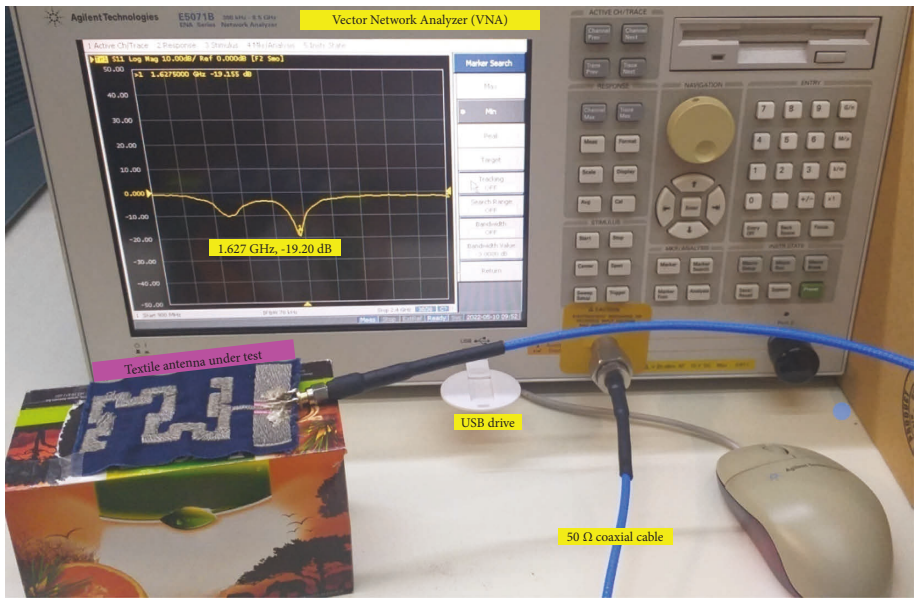

FIGURE 5: Measurement setup for the fabricated textile antenna.

simulations and a very good agreement was obtained providing S11 $-10\,dB$ (i.e., 90% of power fed is delivered) and VSWR < 2, respectively, with an acceptable resonant frequency close to 1.62 GHz.

3.2. Simulated Radiation Pattern and Current Distribution. The radiation pattern of an antenna is a graphical representation of the relative field strength transmitted from or received by the antenna as an angular function of directional coordinates. Usually, it is represented graphically for the far-field properties of an antenna along the electric field (*E*-plane) and the magnetic field (*H*-plane), in the direction of maximum radiation, which are reference planes for linearly-polarized antennas. The *E*-plane determines the polarization of the radio wave, which relates to the orientation of the electric and magnetic components of electromagnetic waves generated from the radiating antenna. It coincides with the azimuth plane for a horizontally polarized antenna and with the elevation plane for a vertically polarized antenna. The opposite is true for the *H*-plane, which is at a right angle to the *E*-plane. Figure 7(a) represents the simulated 3D radiation gain pattern of the proposed antenna at 1.62 GHz. A simulation of the antenna was performed for the range of frequencies from 0.9 GHz to 2.4 GHz, where a maximum gain and radiation efficiency of 3.8 dB and 92.28%, respectively, were obtained. The simulated surface current distribution of the antenna is also given in Figure 7(b),

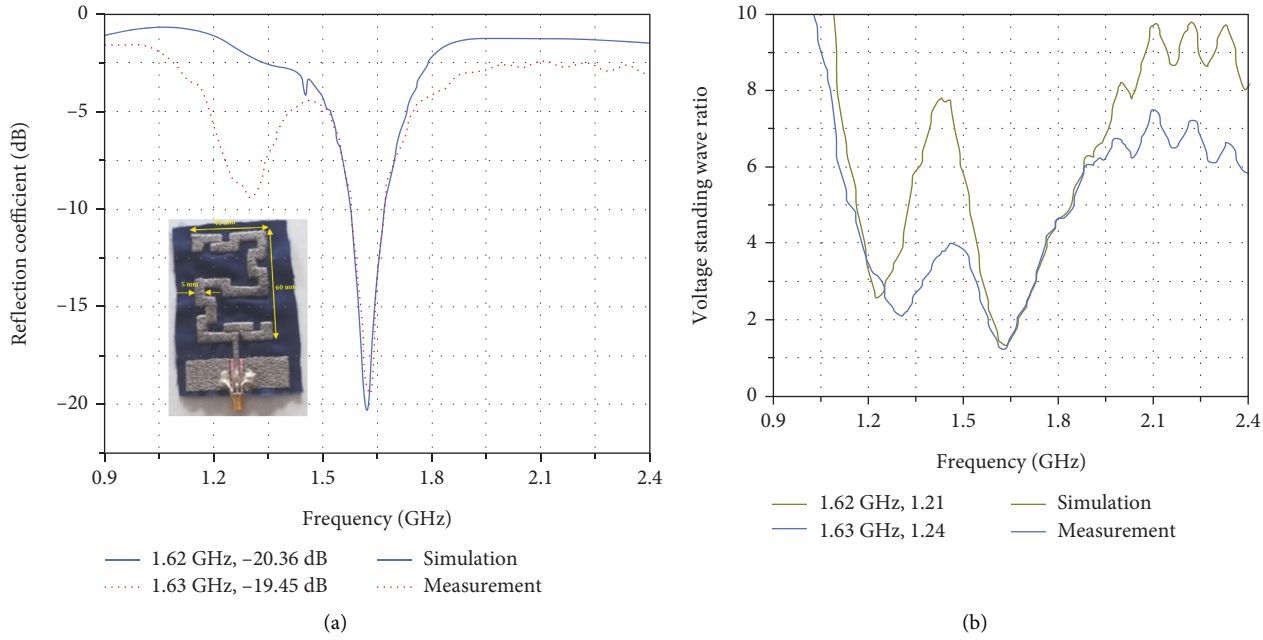

Figure 6: Simulated and measured (a) return loss and (b) VSWR plot for the textile antenna.

indicating the current density and flow of the electric field inside the conducting parts of antenna along with a density meter for multiple frequencies. It can be observed from simulation results that a high strength of current is found to be radiated along the edges of the Z-shaped patch as well as along the transmission line at 1.62 GHz. The corresponding 2D radiation gain patterns on the azimuth plane (i.e., X-Y plane at $\theta = 90^{\circ}$) and the elevation planes (i.e., X-Z plane at $\varphi = 0^{\circ}$ and Y-Z plane at $\varphi = 90^{\circ}$) were simulated as shown in Figures 7(c) and 7(d), respectively, at the operating frequency of 1.62 GHz. It can be seen from the simulated radiation pattern that the designed antenna provides a directional radiation pattern in both planes. In the E-plane (i.e., X-Z plane), there is a single main lobe that is radiated out from the front of the antenna with a fairly wide beamwidth. Part of the radiation is focused around the feed line, which agrees with the current distribution given in Figure 7(b). Furthermore, the radiation pattern for the H-plane (i.e., Y-Z plane) at the resonant frequency demonstrates a radiation pattern similar to a conventional monopole antenna, displaying a directional pattern with two shallow nulls. The designed antenna in this study can be used in applications that do not require a long range, which means it is ideal for body-area network applications.

3.3. Impact of Various Wearability Conditions on Antenna Performance. An embroidered fully-textile antenna proposed in this paper was designed and fabricated to be used as part of normal clothing for radio-frequency (RF) harvesting and for short-range communication purposes in body-area networks for various wearable applications. As such, there will always be an interaction between the antenna and the human body, which is a hostile environment for the propagation of electromagnetic waves. In this section, the performance of the fabricated antenna is studied under different wearability and deployment conditions, such as proximity to the human body, under different bending scenarios, and repeated wet conditions with sweat, in order to validate simulation results and the overall functionality of the proposed textile antenna in the real environment.

3.3.1. Analysis of Fabricated Antenna on Bent Conditions. Flexible and wearable antennas are designed to be used on the human body, which has uneven surfaces, and due to the frequent movements made by the user and the nature of the textile fabric, bending and twisting actions are always unavoidable. Due to these effects, the performance of wearable antennas changes, often negatively, when mounted in garments worn on the human body, such as the arms and thighs. This implies that it is necessary for wearable and flexible antennas to be comfortable for the user, easily integrated into the clothing, as well as robust under different bending and twisting conditions. For this reason, antenna flexibility tests have been carried out by bending the fabricated textile antenna over rolling papers of different diameters, as shown in Figures 8(a)–8(e). Rolling papers with diameters of 120 mm, 100 mm, 80 mm, and 60 mm were chosen by considering the radii of different locations on the human body, where antennas can probably be placed or integrated with the clothing, in order to evaluate the flexibility of the fabricated textile antenna in terms of the resonant frequency and return loss response. The corresponding bending angle (θ) in degree for the textile antenna when it was bended over rolling

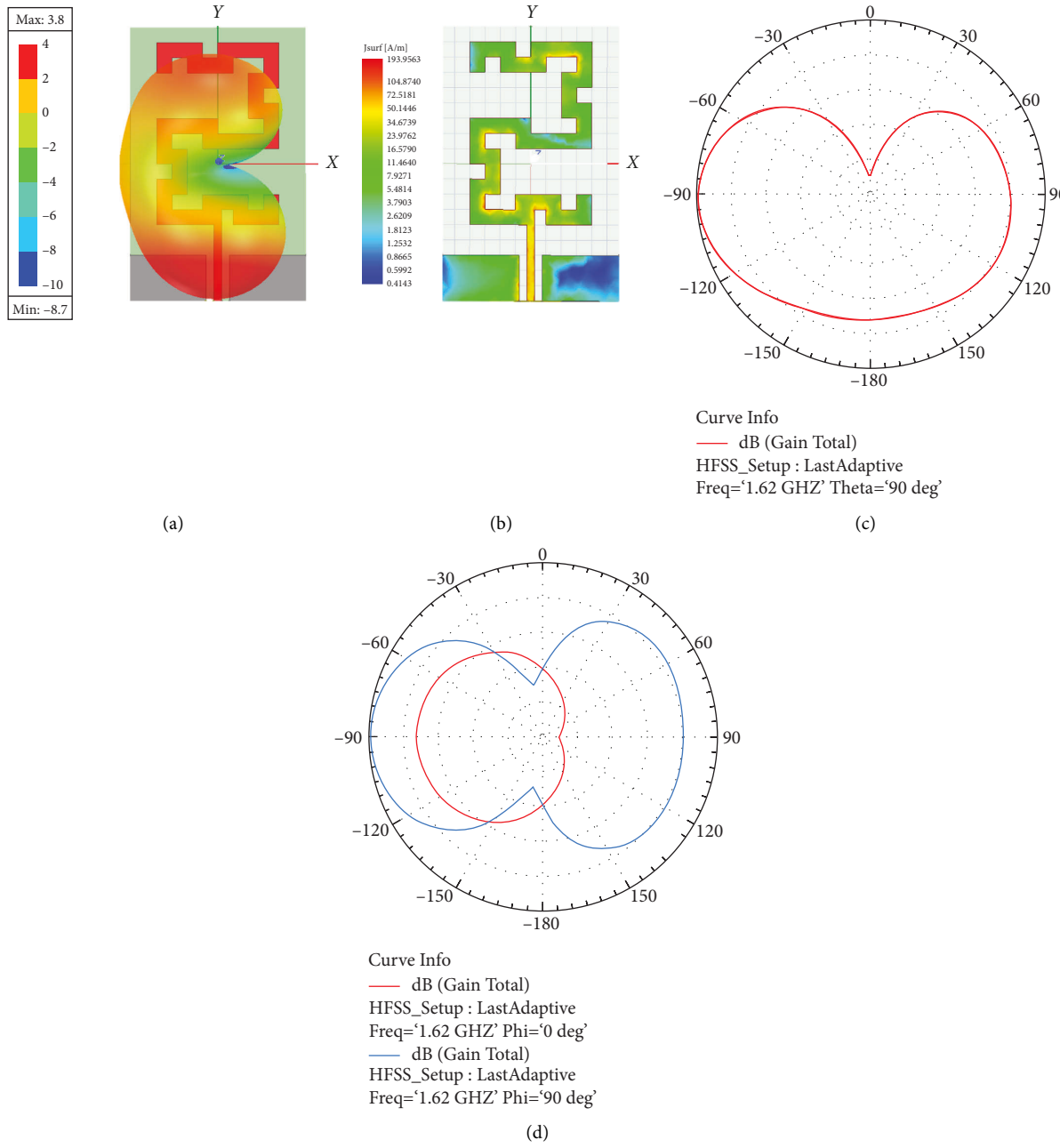

FIGURE 7: (a) Simulated 3D radiation pattern of the antenna, (b) surface current distribution and 2D radiation pattern, (c) over the azimuth plane (*E*-plane), and (d) elevation plane (*H*-plane) for the proposed antenna at 1.62 GHz.

papers of different diameters was computed, using a simple formula as in (8), for the total length, $S = 85\,mm$, of the antenna.

$$\theta(^\circ) = \frac{X}{r} * \frac{180}{\pi}, \tag{8}$$

where X is the total length of the bended portion of the antenna under test and r is the radius of the rolling paper in millimetres, which is computed as half of the corresponding diameter of the rolling paper over which the antenna was bended for testing purposes.

The measured return loss results corresponding to different bending radii (or bending angles) are presented in Figure 9. Due to the bending effect, the resonant length of the antenna usually changes, which further results in a small shift in the operating frequency of the antenna. Significant deviation from the measurement result under the normal flat orientation of the antenna is observed for the highest bending angle, $\theta = 162.34^\circ$ since the rolling paper over which the antenna was bended has the smallest radius of 30 mm. In contrast, the minimum variation in the operating frequency of an antenna is observed for the bending angle of 97.40° (i.e., bending radius of 50 mm). Finally, when the

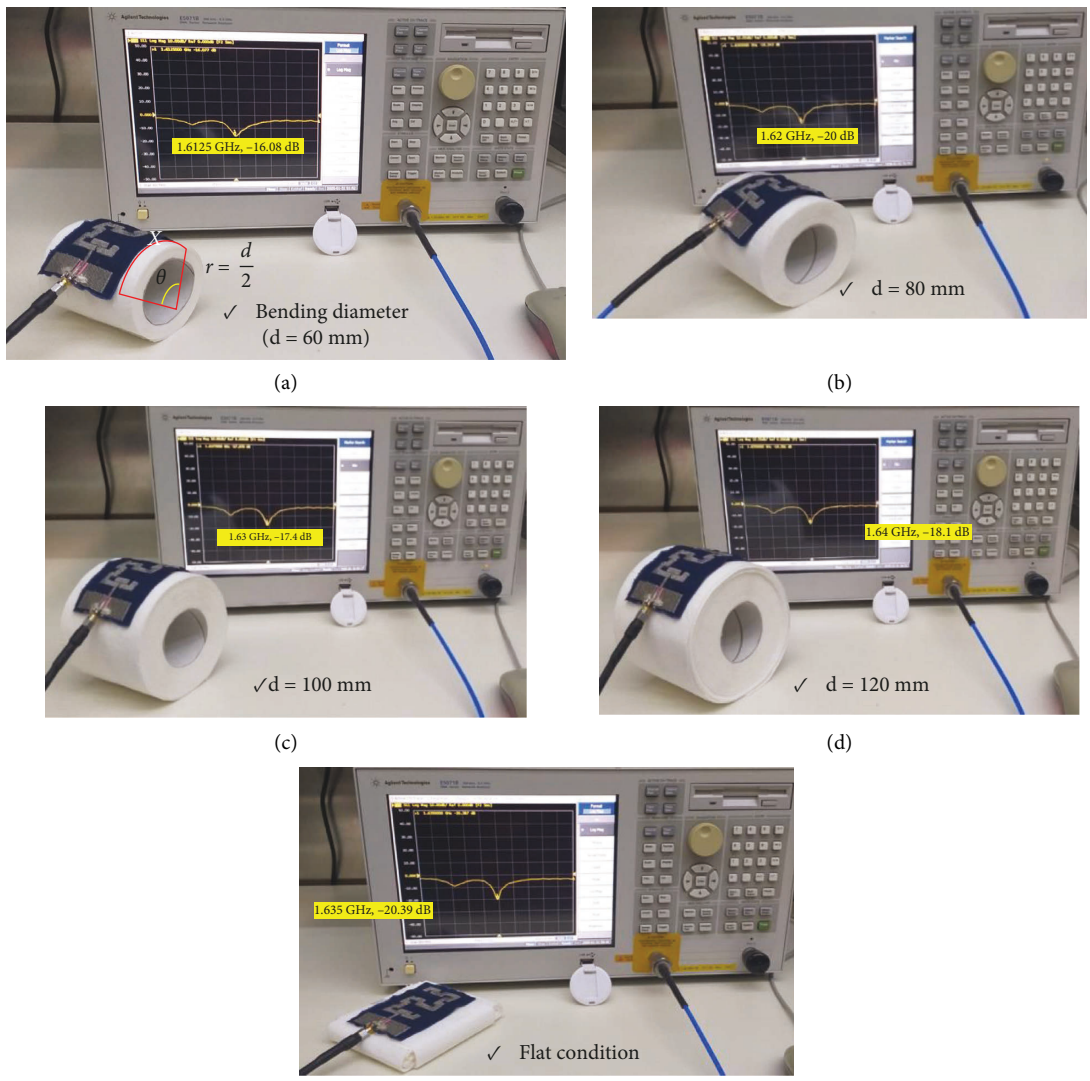

FIGURE 8: Snapshot of measurement setup under different bending angles of the fabricated antenna; (a) bending angle, $\theta = 162.34^{\circ}$, (b) $\theta = 121.75^{\circ}$, (c) $\theta = 97.40^{\circ}$, (d) $\theta = 81.17^{\circ}$, and (e) $\theta = 0.00^{\circ}$.

antenna was bent over the rolling paper with the highest radii (i.e., r = 60 mm), no variation was observed in the operating frequency of the antenna as this scenario was approaching towards the normal flat orientation of the antenna under test.

As it can be observed from Figure 9, the measured resonant frequency spans from 1.61 GHz to 1.64 GHz for the range of bending angles considered. Subsequently, the magnitude of the return loss varies from −22.8 dB to −17.6 dB for the fabricated textile antenna. From the experimental results, it can also be noted that with decreasing in the bending angle (i.e., increasing bending radius), the resonant frequency increases and the antenna tends to reach its operating frequency at the normal flat orientation (i.e., $\theta = 0^{\circ}$). Moreover, a very good agreement was observed between the simulations and measurement results, not only in the normal flat case but also under different bending conditions of the fabricated textile antenna. Overall, the experimental results showed that there were no severe changes in the input-impedance bandwidth of the antenna (i.e., a −10 dB impedance bandwidth of 1.58 GHz to 1.71 GHz) as well as return loss at the operating frequency when the antenna was bent around rolling papers of different radii.

3.3.2. Analysis of Textile Antenna on Sweat Conditions. Sweat is an easily accessible and attractive source of information. For example, to detect and monitor a user's unsafe levels of alcohol consumption lifestyle in a noninvasive way, which increases rapidly worldwide, leading to serious health concerns and significant socioeconomic costs. Moreover, sweat is an ideal bio-fluid that can be collected noninvasively and without the requirement of active participation of the person to perform measurements in real-time. Accordingly, artificial sweat was applied, in steps of 10 μL to a maximum of 50 μL, at the same place on the conducting parts of the antenna, using a micropipette as shown in Figure 10(a).

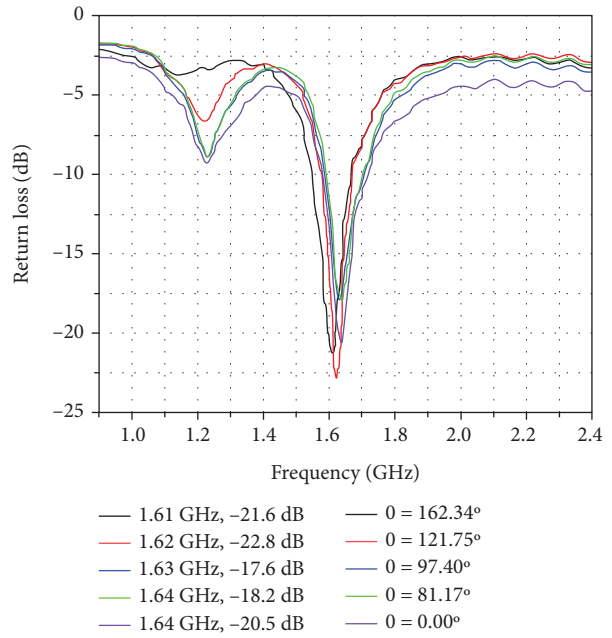

Figure 9: Measured return loss versus frequency plot for textile antenna under bending conditions.

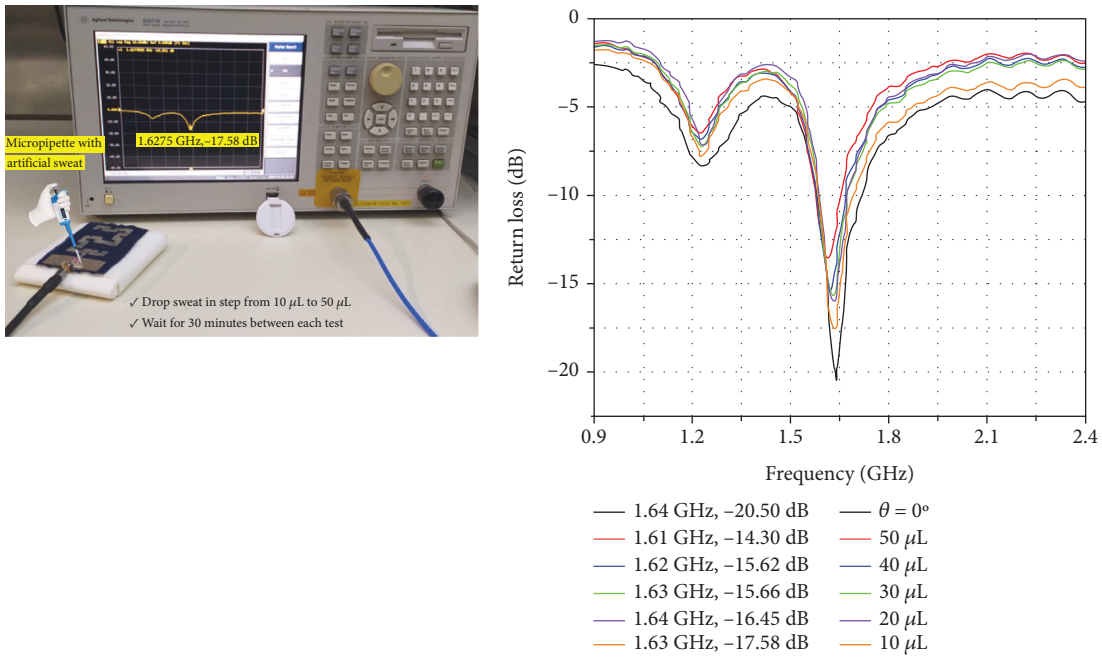

Figure 10: (a) A snapshot of the measurement setup in the wet condition of the antenna; and (b) return loss versus frequency plot when the antenna gets wetted with different quantities of artificial sweat.

Antenna performance was measured in terms of the return loss (dB) with 30 minutes of waiting time between each test. At first, 10 μL of artificial sweat was applied to the fabricated textile antenna, and a return loss of −17.58 dB was obtained at 1.63 GHz. After 30 minutes of waiting time, another 20 μL of artificial sweat was applied at the same place and a return loss of −16.45 dB was obtained at 1.64 GHz. Similarly, 30 μL, 40 μL, and 50 μL of artificial sweat samples were applied to the antenna in the same way, where the return loss values of −15.66 dB, −15.62 dB, and −14.30 dB at the operating frequencies of 1.6275 GHz, 1.62 GHz, and 1.6125 GHz were obtained, respectively, as depicted in Figure 10(b).

As it can be seen from Figure 10(b), the operating frequency changes very little even after repeated wet conditions with sweat, which mimic the realistic situation when the antenna is mounted in different wearables and body-

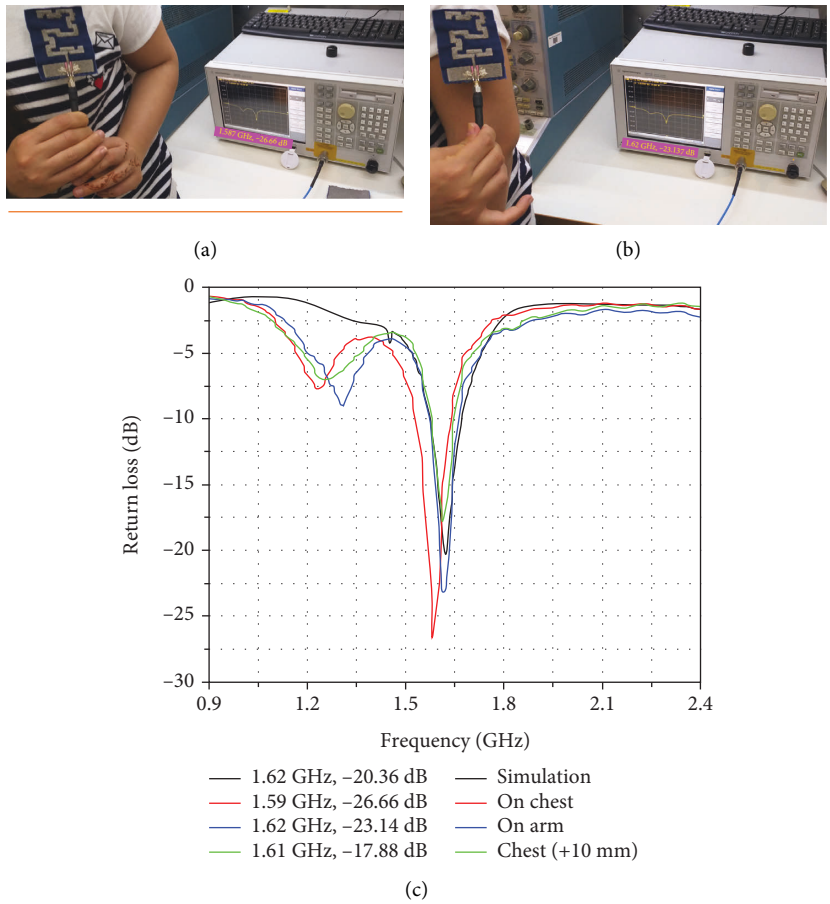

Figure 11: (a) Fabricated textile antenna placed on the chest, (b) conformal on the human arm for experimental study of the body's effect on antenna performance, and (c) return loss versus frequency plot.

worn garments. However, the shift in the resonant frequency stays within the operational bandwidth of the antenna (i.e., within a −10 dB impedance bandwidth of 1.58 GHz to 1.71 GHz). This confirms that the proposed fully-textile antenna can be easily deployed on working clothes or undergarments and will still continue to communicate effectively.

3.3.3. Analysis of Antenna in Proximity with the Human Body. Experimental study of the fabricated textile antenna was performed in proximity with the human body by placing the antenna on the chest and conformal on the human arm as depicted in Figures 11(a) and 11(b). Antenna performance was investigated by means of measurement of the reflection coefficient (dB) while the antenna was kept on the chest, at 10 mm distance from the human chest, as well as by placing it conformal on the arm of the human body.

It can be observed, from the experimental results in Figure 11(c), that the fabricated antenna was able to provide a return loss below −10 dB, indicating its good performance when placed in a close proximity with the human body. Even though there are slight variations in the resonant frequency, the change is very little and it stays within the simulated operational bandwidth of the antenna (1.58 GHz to 1.68 GHz). Moreover, from the previous experimental results in Figure 9, the return loss ratio when the antenna was bent over the rolling paper of radius 40 mm (i.e., $\theta = 121.75^{\circ}$), corresponding to the radius of a human arm, to the return loss in the normal flat case is 0.9878. A similar analysis of the return loss ratio was performed for the on-body condition of the antenna as shown in Figures 11(a) and 11(b). Accordingly, the ratio of return loss when the antenna was placed on the human arm to the value when placed on the human chest, as shown in Figure 11(c), is approximately 98%. This implies that the on-body behaviour of the antenna is not very different from without a body, and the proposed textile antenna can be easily integrated into smart clothing applications and effectively work together with the on-body communication devices over a short range.

The novelty of this work lies in all the processing stages involved. At first, the conducting parts were designed only on one side of the substrate; hence, fabrication was made on a single layer of cotton textile, which is naturally safe and comfortable to wear. This makes the proposed antenna highly conformal to the body and ergonomic to accommodate daily human movement. Moreover, an embroidery technique using silver conductive threads was employed for fabrication with

Table 2: Summary of the novelty of the present work compared with previous works.

Method of design	Fabrication method	Reference
Additional layers were between the patch and ground	Using embroidery on two different layers	[31, 32]
Patch and ground designed on the same side of the antenna	On a single-layer textile using an embroidery	Present work

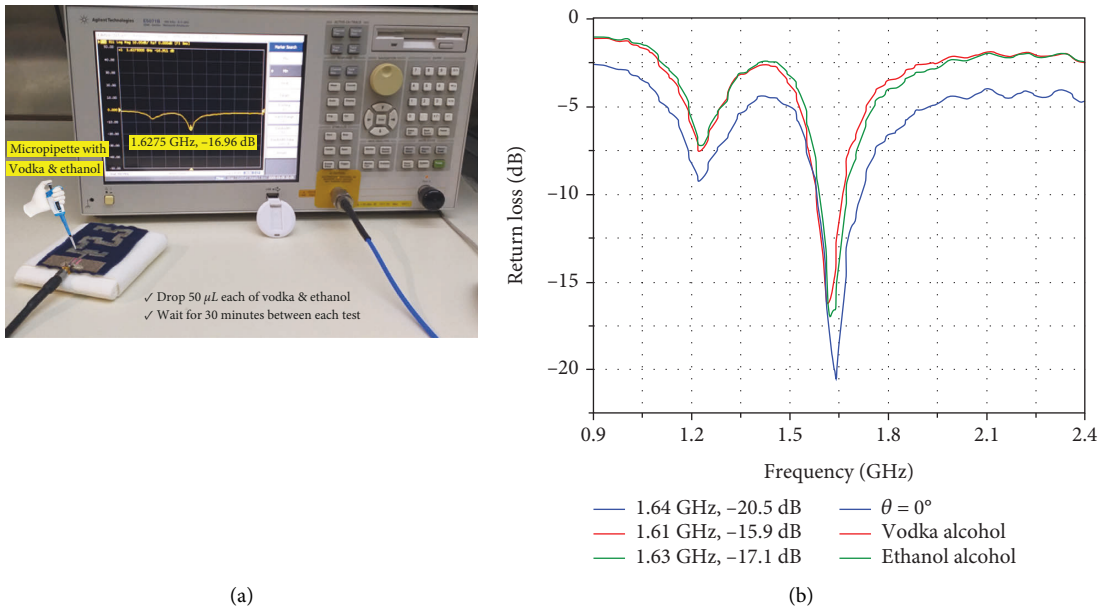

Figure 12: (a) Snapshot of measurement setup under accidental spills, and (b) return loss plot of the proposed textile antenna when wetted with 50 μL each of ethanol alcohol and vodka alcohol.

no additional adhesive materials and rigid electronic components. Finally, characterization was performed under different deployment conditions to ascertain its functionality in a real environment, and overall, the antenna showed optimal performance. Table 2 summarizes the novelty of the present work in terms of design and fabrication techniques.

3.3.4. Antenna Response under the Exposure to Accidental Spills. In order to make sure that the antenna still works effectively under accidental spills of liquids, the fabricated textile antenna was studied under exposure to ethanol alcohol (70% v/v) and vodka alcohol (40% v/v), which mimic the realistic on-body conditions. Antenna performance was investigated by measuring the return loss (dB) response. Accordingly, the same quantity of ethanol alcohol and vodka alcohol was applied, as depicted in Figure 12(a), at the same place on the conducting parts of the antenna, using a micropipette. The measurement of S11 (dB) was performed with 30 minutes of waiting time between each test. At first, 50 μL of ethanol alcohol was applied, where a return loss of −17.06 dB was observed at the operating frequency of 1.6275 GHz. Then, after 30 minutes of waiting time, another 50 μL of vodka alcohol was applied at the same place, and a return loss of −15.9 dB was obtained at 1.6125 GHz.

The return loss plot for the fabricated textile antenna, when wetted with 50 μL each of ethanol alcohol and vodka alcohol, was analysed and comparisons with the dry measurement condition were made as depicted in Figure 12(b). There are slight variations in the operating frequency of the antenna compared to the previously dry measurement scenario (i.e., $\theta = 0^{\circ}$) as shown in Figure 9. However, the change is very small and the results stay within the simulated operational bandwidth of the antenna (1.58 GHz to 1.68 GHz). This shows the optimal performance of the proposed textile antenna even under exposure to accidental spillage of liquids such as ethanol and vodka alcohol.

4. Conclusions

In this work, an embroidered CPW–fed meander line *Z*-shaped monopole textile antenna for radio-frequency (RF) harvesting and for short-range communication purposes in the body-area network for various wearable applications was presented. The antenna was designed and fabricated on a cost-effective and commercially available woven cotton textile cloth, where the conducting parts were made of silver conductive thread (silver–tech 50) using a digital embroidery technique. The performance of the antenna was investigated in close proximity to the human body, under exposure to accidental spills and repeated wet conditions with sweat, as well as under different bending angles corresponding to the radii of various locations of the human body where antennas can probably be placed or integrated with the clothing. It was found that the properties of the fabricated textile antenna do not change significantly. Even though there are small discrepancies in terms of operating frequency and impedance bandwidth, which can be

attributed to the bending and soldering effects, a very good agreement between the simulations and measurement results of return loss at 1.62 GHz frequency was obtained. Overall, the fabricated compact and flexible fully-textile embroidered antenna performed well, which makes it suitable for future high-performance wearable smart clothing applications.

The design and fabrication of miniaturized textile antennas for high-frequency body-area network applications are envisioned for future work by changing dimensions from the already fabricated antenna prototype. Even though various flexible and textile antenna works have been reported in the scientific literature, it is still a long way for wearable textile antennas to improve their performance and increase reliability in future Internet-of-bodies (IoB) related applications. Further research is still needed to explore novel antenna designs, compatible fabrication and feeding techniques, as well as integration of high-frequency systems into clothing to make a real wearable, washable, and entirely textile antenna, which is insensitive to bending as well as to the proximity of the human body as well as energy harvesting aspects.

Data Availability

Data will be made available upon request to the corresponding author.

Conflicts of Interest

The authors declare that there are no conflicts of interest.

Acknowledgments

This study has received funding from the European Union's Horizon 2020 Research and Innovation Programme under grant agreement (no. 854194). A. E. A. would like to thank Dr. Milan Radovanovic for the training in VNA.

References

[1] A. Vahora and K. Pandya, "Microstrip feed two elements pentagon dielectric resonator antenna array," in *Proceedings of the International Conference on Innovative Trends and Advances in Engineering and Technology (ICITAET)*, Shegoaon, India, December 2019.

[2] A. Vahora and K. Pandya, "Triple band dielectric resonator antenna array using power divider network technique for gps navigation/bluetooth/satellite applications," *International Journal of Microwave and Optical Technology*, vol. 15, pp. 369–378, 2020.

[3] N. Rais, P. J. Soh, F. Malek, S. Ahmad, N. B. M. Hashim, and P. S. Hall, "A review of wearable antenna," in *Proceedings of the 2009 Loughborough antennas & propagation conference*, IEEE, Loughborough, UK, November 2009.

[4] P. S. Hall and Y. Hao, "Antennas and propagation for body centric communications," in *Proceedings of the 2006 First European Conference on Antennas and Propagation*, IEEE, Nice, France, November 2006.

[5] L. Wang, Z. Lou, K. Jiang, and G. Shen, "Bio-multifunctional smart wearable sensors for medical devices," *Advanced Intelligent Systems*, vol. 1, no. 5, Article ID 1900040, 2019.

[6] Y. Li, Z. Zhang, Z. Feng, and H. R. Khaleel, "Fabrication and measurement techniques of wearable and flexible antennas," *Cult Tour*, vol. 1, pp. 7–23, 2014.

[7] T. Upadhyaya, R. Patel, A. Desai, U. Patel, K. Pandya, and K. P. Kaur, "Electrically tilted broadband antenna using negative refractive index material," in *Proceedings of the Third International conference on I-SMAC (IoT in Social, Mobile, Analytics and Cloud) (I-SMAC)*, pp. 685–689, Palladam, India, December 2019.

[8] S. Varma, S. Sharma, M. John, R. Bharadwaj, A. Dhawan, and S. K. Koul, "Design and performance analysis of compact wearable textile antennas for iot and body-centric communication applications," *International Journal of Antennas and Propagation*, vol. 2021, Article ID 7698765, 12 pages, 2021.

[9] W. Scanlon, G. Conway, and S. Cotton, "Antennas and propagation considerations for robust wireless communications in medical body area networks," in *Proceedings of the IET Seminar on Antennas and Propagation for Body-Centric Wireless Communications*, London, UK, April 2007.

[10] A. Kiourti and K. S. Nikita, "A review of implantable patch antennas for biomedical telemetry: challenges and solutions [wireless corner]," *IEEE Antennas and Propagation Magazine*, vol. 54, no. 3, pp. 210–228, 2012.

[11] N. Chahat, M. Zhadobov, L. Le Coq, and R. Sauleau, "Wearable endfire textile antenna for on-body communications at 60 ghz," *IEEE Antennas and Wireless Propagation Letters*, vol. 11, pp. 799–802, 2012.

[12] B. Ivšić, J. Bartolić, D. Bonefačić, A. Skrivervik, and J. Trajkovik, "Design and analysis of planar uhf wearable antenna," in *Proceedings of the 2012 6th European Conference on Antennas and Propagation*, IEEE, Prague, Czech Republic, March 2012.

[13] S. M. Ali, C. Sovuthy, S. Noghanian et al., "Design and evaluation of a flexible dual-band meander line monopole antenna for on- and off-body healthcare applications," *Micromachines*, vol. 12, no. 5, p. 475, 2021.

[14] J. Yeo and J. I. Lee, "Meander-line slot-loaded high-sensitivity microstrip patch sensor antenna for relative permittivity measurement," *Sensors*, vol. 19, no. 21, p. 4660, 2019.

[15] K. Pandya, T. Upadhyaya, U. Patel, and A. Pandaya, "Ring shape dielectric resonator antenna for wlan application," *International Journal of Creative Research Thoughts*, vol. 9, no. 12, 2021.

[16] K. Viswanadha and N. S. Raghava, "Design and analysis of a meander line cornered microstrip patch antenna with square slotted ebg structure for ism/wlan applications," *International Journal of Advanced Science and Technology*, vol. 113, pp. 93–102, 2018.

[17] N. Zainuddin, Z. Zakaria, M. Abd Aziz, M. N. Husain, and M. A. Mutalib, "Investigation of meander slots to microstrip patch patch antenna," in *Proceedings of the 2013 IEEE InM. N. Husain; M. A. Mutalibternational Conference on RFID-Technologies and Applications (RFID-TA)*, IEEE, ohor Bahru, Malaysia, September 2013.

[18] R. Bharadwaj and S. K. Koul, "Assessment of limb movement activities using wearable ultra-wideband technology," *IEEE Transactions on Antennas and Propagation*, vol. 69, no. 4, pp. 2316–2325, 2021.

[19] M. Monirujjaman Khan, J. Hossain, K. Islam et al., "Design and study of an mmwave wearable textile based compact antenna for healthcare applications," *International Journal of*

Antennas and Propagation, vol. 2021, Article ID 6506128, 2117 pages, 2021.

[20] M. El Gharbi, R. Fernández-García, S. Ahyoud, and I. Gil, "A review of flexible wearable antenna sensors: design, fabrication methods, and applications," *Materials*, vol. 13, no. 17, p. 3781, 2020.

[21] S. G. Kirtania, A. W. Elger, M. R. Hasan et al., "Flexible antennas: a review," *Micromachines*, vol. 11, no. 9, p. 847, 2020.

[22] H. R. Khaleel, H. M. Al-Rizzo, D. G. Rucker, and S. Mohan, "A compact polyimide-based uwb antenna for flexible electronics," *IEEE Antennas and Wireless Propagation Letters*, vol. 11, pp. 564–567, 2012.

[23] A. Yadav, V. Kumar Singh, A. Kumar Bhoi, G. Marques, B. Garcia-Zapirain, and I. de la Torre Diez, "Wireless body area networks: uwb wearable textile antenna for telemedicine and mobile health systems," *Micromachines*, vol. 11, no. 6, p. 558, 2020.

[24] M. Ur-Rehman, T. Kalsoom, N. A. Malik et al., "A wearable antenna for mmwave iot applications," in *Proceedings of the 2018 IEEE International Symposium on Antennas and Propagation & USNC/URSI National Radio Science Meeting*, IEEE, Boston, MA, USA, July 2018.

[25] J. Pourahmadazar and T. A. Denidni, "60 ghz antenna array for millimeter-wave wireless sensor devices using silver nanoparticles ink mounted on a flexible polymer substrate," *Microwave and Optical Technology Letters*, vol. 59, no. 11, pp. 2830–2835, 2017.

[26] K. Karlsson and J. Carlsson, Eds., in *Proceedings of the 2012 6th European Conference on Antennas and Propagation*, IEEE, Prague, Czech Republic, March 2012.

[27] Y. Ouyang and W. J. Chappell, "High frequency properties of electro-textiles for wearable antenna applications," *IEEE Transactions on Antennas and Propagation*, vol. 56, no. 2, pp. 381–389, 2008.

[28] P. M. Potey and K. Tuckley, "Design of wearable textile antenna with various substrate and investigation on fabric selection," in *Proceedings of the 2018 3rd international conference on microwave and photonics*, IEEE, Dhanbad, India, February 2018.

[29] A. Tsolis, W. G. Whittow, A. A. Alexandridis, and J. Vardaxoglou, "Embroidery and related manufacturing techniques for wearable antennas: challenges and opportunities," *Electronics*, vol. 3, no. 2, pp. 314–338, 2014.

[30] A. Alemaryeen and S. Noghanian, "Amc integrated textile monopole antenna for wearable applications," *Applied Computational Electromagnetics Society Journal*, vol. 31, pp. 612–618, 2016.

[31] M. A. R. Osman, M. K. Abd Rahim, N. A. Samsuri, H. A. M. Salim, and M. F. Ali, "Embroidered fully textile wearable antenna for medical monitoring applications," *Progress In Electromagnetics Research*, vol. 117, pp. 321–337, 2011.

[32] A. Anbalagan, E. F. Sundarsingh, and V. S. Ramalingam, "Design and experimental evaluation of a novel on-body textile antenna for unicast applications," *Microwave and Optical Technology Letters*, vol. 62, no. 2, pp. 789–799, 2020.

[33] D. Misman, I. A. Salamat, M. F. A. Kadir, M. R. Che Rose, M. S. R. Mohd Shah, and M. Z. A. Abd Aziz, "The effect of conductor line to meander line antenna design," in *Proceedings of the 2008 Loughborough Antennas and Propagation Conference*, Melaka, Malaysia, December 2008, https://ieeexplore.ieee.org/author/37312538600.

[34] C. Mukta, M. Rahman, and A. Z. M. T. Islam, "Design of a compact circular microstrip patch antenna for wlan applications," *International Journal on AdHoc Networking Systems*, vol. 11, no. 3, pp. 01–11, 2021.

[35] Rachmansyah, A. Irianto, and A. B. Mutiara, "Designing and manufacturing microstrip antenna for wireless communication at 2.4 ghz," *International Journal of Computer and Electrical Engineering*, vol. 3, pp. 670–675, 2011.

[36] D. Bhalla, "Design of a rectangular microstrip patch antenna using inset feed technique," *IOSR Journal of Electronics and Communication Engineering*, vol. 7, no. 4, pp. 08–13, 2013.

[37] I. Codreanu and G. D. Boreman, "Influence of dielectric substrate on the responsivity of microstrip dipole-antenna-coupled infrared microbolometers," *Applied Optics*, vol. 41, no. 10, pp. 1835–1840, 2002.

[38] A. Elrashidi, K. Elleithy Hassan Bajwa, and H. Bajwa, "Input impedance, vswr and return loss of a conformal microstrip printed antenna for tm01 mode using two different substrates," *International Journal of Networks and Communications*, vol. 2, pp. 13–19, 2012.

[39] D. Pozar, *Microwave engineering*, vol. 2, 2004.

[40] P. G. Paga, H. C. Nagaraj, and T. S. Rukmini, "Design Simulation and Fabrication of a Dual Band Frequency Reconfigurable Monopole Antenna for Wi-Fi and Wimax Applications," *Open Journal of Antennas and Propagation*, vol. 5, 2017.

[41] I. H. Daniel, J. A. Flint, and R. D. Seager, "Stitched transmission lines for wearable rf devices," *Microwave and Optical Technology Letters*, vol. 59, no. 5, pp. 1048–1052, 2017 05/01.

[42] B. Ivsic, D. Bonefacic, and J. Bartolic, "Considerations on embroidered textile antennas for wearable applications," *IEEE Antennas and Wireless Propagation Letters*, vol. 12, pp. 1708–1711, 2013.